

High-efficiency beam-wave interaction in quasiperiodic structures

Levi Schächter

Department of Electrical Engineering, Technion-Israel Institute of Technology, Haifa 32000, Israel

(Received 5 December 1994)

A semianalytical method for the design and analysis of high-efficiency (> 50%) generation of radiation in traveling output structures is presented. No *a priori* assumption about the functional form of the electromagnetic field is required. The concept of scalar interaction impedance used in periodic structures is generalized to a matrix in the case of a nonperiodic system. Its eigenvalue is shown to be directly related to the beam-wave interaction efficiency. The method is demonstrated with the design and analysis of a 70% efficiency system.

PACS number(s): 52.75.Ms, 03.40.Kf

INTRODUCTION

A substantial effort in the investigation of high power radiation sources has been directed towards improving the efficiency. Traveling wave output sections [1–4] play an important role in these devices due to the distributed interaction, which permits high efficiency with low gradients on the metallic surface, and consequently, lower probability of rf breakdown. In the context of high power devices, a traveling wave output section consists of a set of coupled cavities with one or more output arms, and it is driven by an initially bunched beam generated by either a klystron or a traveling wave tube.

The beam-wave interaction in periodic traveling wave tubes relies on synchronism of the average velocity of the electrons with the phase velocity of the interacting wave. Systems with uniform structures can generate rf at power levels that may correspond to 5–12% efficiency in a single stage amplifier [5] or 40% in a two stage system [6–8]. The efficiency of a uniform structure is higher as the electrons are more relativistic; however, the volume and cost of electron generators limit the output energies to less than 1 MeV, and in many cases even below 500 keV. If we consider the latter case, the initial velocity is $V=0.86c$; thus for an 80% efficiency system, the synchronism condition at the output would require a phase velocity of $0.55c$; this corresponds to a 36% change in the phase velocity. In order to achieve this variation, a similar relative change in the geometry will be required, and consequently, the system is no longer periodic. The geometry variations mentioned above should not affect the transmission or reflection characteristics of the structure; otherwise, sidebands occur, the interaction saturates, and not less severe, the system is prompt to oscillate [9].

Spatial variations of periodic structures are used in acceleration modules in order to adapt the interaction impedance to the local power that flows in the system. The interaction impedance is a measure of the longitudinal electric field, which acts on the electron (E) at a total electromagnetic power (P) flowing in the waveguide, $Z_{\text{int}} \propto |E|^2/P$. Perturbation from periodicity in acceleration modules occurs over many periods of the structure,

and it is designed for minimum reflections. In a regular periodic structure, at a given frequency and single mode operation, the electromagnetic wave is characterized by a single wave number k , and quantities such as phase velocity, group velocity, and interaction impedance are well defined. In principle, once the structure is no longer periodic the field cannot be represented by a single wave number. However, in the case of adiabatic variations these characteristics of the structure (phase velocity, group velocity, and interaction impedance) are assumed to be determined entirely by the geometry of the local cell.

This is not the case in traveling wave output sections, where variations typically occur in one wavelength of the radiation field. This nonadiabatic change of geometry dictates a wide spatial spectrum in which case the formulation of the interaction in terms of a single wave with a varying amplitude and phase is inadequate; in fact, the electromagnetic field cannot be expressed in a simple (analytic) form if substantial geometric variations occur from one cell to another. To be more specific, in a uniform or weakly tapered disk loaded waveguide, the beam-wave interaction is analyzed assuming that the general functional form of the electromagnetic wave is known, i.e., $A(z)\cos[\omega t - kz - \phi(z)]$ and the beam affects [10] only the amplitude $A(z)$ and the phase, $\phi(z)$. Furthermore, it is assumed that the variation due to the interaction is small on the scale of one wavelength of the radiation. Both assumptions are not acceptable in the case of a structure designed for high-efficiency interaction.

In order to emphasize the difficulty even further, we recall that a nonadiabatic local perturbation of geometry affects *global* electromagnetic characteristics; that is to say that a change in a given cell affects the interaction impedance or the group velocity several cells before and after the point where the geometry was altered. For comparison, in a free electron laser, a local change in the ponderomotive force affects *locally* the interaction [11].

In order to optimize these conflicting requirements we have developed an analytical technique that permits us to design a quasiperiodic structure. It relies on a model that consists of a cylindrical waveguide to which a set of pill-

box cavities and a radial arm are attached. In principle the number of cavities and arms is arbitrary. The boundary condition problem is formulated in terms of the amplitudes of the electromagnetic field in the cavities and arms. The elements of the matrix that relate these amplitudes to the source term are analytic functions; thus, no *a priori* knowledge of the functional behavior of the electromagnetic field is necessary. In previous studies [12,13] we examined the homogeneous electromagnetic characteristic of quasiperiodic structures; the technique was further developed to include Green's function and the beam-wave interaction within the framework of the linear hydrodynamic approximation for the beam dynamics. It was shown that the method [13] combines the features of beam-gap (local) interaction, as in a klystron, with those of beam-wave (distributed) interaction in a traveling wave structure. The linearity of the model above is a serious limitation for a high-efficiency interaction, since it is valid only for a small variations from the initial average velocity. For this reason, the tools developed previously are used in the present study to formulate the beam-wave interaction within the framework of a macroparticle dynamics, which permits a description of large deviation from average velocity. It is shown that the interaction is controlled by a *matrix interaction impedance*, which can be conceived as a generalization of the scalar interaction impedance concept, introduced for uniform structures. Its definition is possible after instead of using a *k*-space decomposition (e.g., Floquet harmonics for periodic structure), we chose to represent the interaction in terms of *z*-space functions. The number of functions is determined by the number of apertures and number of modes that represent, at the required accuracy, the electromagnetic field in the grooves and arms. Each function has its peak at a different aperture; however, the functions are not orthogonal. The matrix interaction impedance is closely related to Green's function of the system in the representation of this set of functions. After we establish the basic formalism we illustrate the design and analysis of a high-efficiency (70%) traveling wave section, including space-charge effects.

DEFINITION OF THE MODEL

A schematic of the system is presented in Fig. 1. It consists of a cylindrical waveguide of radius R_{int} to which an arbitrary number of pill-box cavities and an output arm are attached; the width of each one is denoted by d_n , where $n = 1, 2, \dots, N$ and N is the total number of cells and arms. The external radius ($R_{\text{ext},n}$) may vary from one cavity to another but the internal radius (R_{int}) has to be constant. The system is driven by a modulated beam that is guided by a very strong ("infinite") magnetic field; thus the motion of the electrons is confined to the z direction. Consequently, in the inner cylinder ($0 < r < R_{\text{int}}$) the current density distribution is entirely in this direction; i.e., $\mathbf{J}(r, z; t) = J_z(r, z; t)\mathbf{1}_z$ and

$$J_z(r, z; t) = -e \sum_i V_i(t) \delta[z - z_i(t)] \frac{1}{2\pi r} \delta(r - r_i(t)); \quad (1)$$

$-e$ is the charge of one electron. In this expression $r_i(t)$

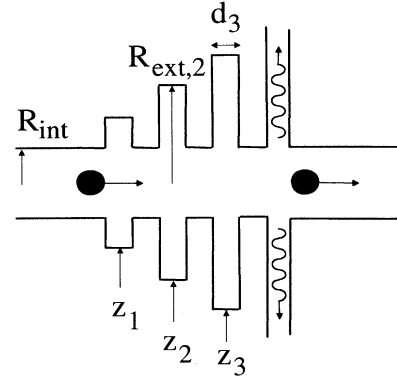


FIG. 1. Schematic of the system under consideration. The external radius R_{ext} , the groove and arm width d , and the separation between any two cavities can be arbitrary; however, the internal radius R_{int} has to be maintained the same. The system is driven by a bunched beam.

and $z_i(t)$ are the location of the i th particle at time t , subject to the assumptions above $r_i(t) = r_i(0)$.

The operation of the system as an amplifier dictates single frequency operation; thus the time dependence of all electromagnetic field components is assumed to be sinusoidal ($e^{j\omega t}$); this tacitly implies that all of the transients associated with the front of the beam have decayed, and for a particular phase-space distribution of electrons, the system can reach the steady state. According to the assumptions above, the time Fourier transform of the current density is

$$J_z(r, z; \omega) = \frac{1}{T} \int_0^T dt e^{-j\omega t} J_z(r, z; t); \quad (2)$$

$T = 2\pi/\omega$ is the period of the wave. This expression can be simplified if no electrons are reflected. For this purpose we denote by $\tau_i(z)$ the time it takes the i th particle to reach the point z in the interaction region and by $V_i(z)$ the velocity of the i th particle at z ; the two are related through

$$\tau_i(z) = \tau_i(0) + \int_0^z d\xi \frac{1}{V_i(\xi)}; \quad (3)$$

$\tau_i(0)$ is the time the i th particle reaches the $z=0$ point chosen to be in the center of the first aperture. Using these definitions the integral in Eq. (2) can be evaluated analytically, and the result is

$$J_z(r, z; \omega) = \frac{-e}{2\pi r T} \sum_i^{N_0} e^{-j\omega\tau_i(z)} \delta[r - r_i(0)]. \quad (4)$$

The summation is over all electrons (N_0) present in one (time) period of the wave, and $I = eN_0/T$ is the average current. It is convenient to average over the transverse direction; thus, by denoting with R_b the beam radius and assuming that the electrons are uniformly distributed on the beam cross section we find that

$$J(z) \equiv \frac{2}{R_b^2} \int_0^{R_b} dr r J_z(r, z; \omega) = -\frac{I}{\pi R_b^2} \langle e^{-j\omega\tau_i(z)} \rangle, \quad (5)$$

where $\langle \rangle \equiv N_0^{-1} \sum_i^{N_0} \dots$. Finally, subject to the previous assumptions, the current density distribution reads

$$J_z(r, z; \omega) = -\frac{I}{\pi R_b^2} \langle e^{-j\omega\tau_i(z)} \rangle h(R_b - r), \quad (6)$$

with $h(x)$ the Heaviside step function; in what follows we shall refer to $\langle e^{-j\omega\tau_i(z)} \rangle$ as the normalized current density.

The longitudinal electric field averaged over the beam cross section, i.e.,

$$E(z) = \frac{2}{R_b^2} \int_0^{R_b} dr r E_z(r, z; \omega), \quad (7)$$

determines the dynamics of the particles via the single particle equation of motion, which in our case coincides with the single particle energy conservation

$$\frac{d}{dz} \gamma_i(z) = -\frac{1}{2} \frac{e}{mc^2} [E(z) e^{j\omega\tau_i(z)} + \text{c.c.}]; \quad (8)$$

m is the rest mass of the electron. In the next section we shall determine the relation between the longitudinal electric field [averaged over the beam cross section, Eq. (7)] and the current density [Eq. (6)].

ELECTROMAGNETIC PROBLEM

The current distribution introduced above excites the longitudinal component of the magnetic vector potential, which satisfies

$$\left[\nabla^2 + \frac{\omega^2}{c^2} \right] A_z(r, z; \omega) = -\mu_0 J_z(r, z; \omega) \quad (9)$$

in the cylindrical waveguide and

$$\left[\nabla^2 + \frac{\omega^2}{c^2} \right] A_z(r, z; \omega) = 0 \quad (10)$$

in the grooves and output arm; in both cases the Lorentz gauge was tacitly assumed. The solution of the magnetic vector potential in the first region ($0 < r < R_{\text{int}}$) reads

$$\begin{aligned} A_z(r, z; \omega) &= 2\pi\mu_0 \int_0^{R_b} dr' r' \int_{-\infty}^{\infty} dz' G_\omega(r, z | r', z') J_z(r', z'; \omega) \\ &\quad + \int_{-\infty}^{\infty} dk A(k) e^{-jkz} I_0(\Gamma r), \end{aligned} \quad (11)$$

where $\Gamma^2 = k^2 - (\omega/c)^2$, $G_\omega(r, z | r', z')$ is the vacuum Green's function:

$$G_\omega(r, z | r', z') = \int_{-\infty}^{\infty} dk e^{-jk(z-z')} g_{\omega, k}(r | r') \quad (12)$$

and

$$g_{\omega, k}(r | r') = \frac{1}{(2\pi)^2} \times \begin{cases} I_0(\Gamma r) K_0(\Gamma r') & \text{for } 0 \leq r < r', \\ K_0(\Gamma r) I_0(\Gamma r') & \text{for } r' \leq r < \infty. \end{cases} \quad (13)$$

$I_0(z)$ and $K_0(x)$ are the zero order modified Bessel function of the first and second kind, respectively. Due to the

azimuthal symmetry of the current distribution and the metallic structure, only symmetric transverse magnetic (TM) modes have been considered.

In the grooves the electromagnetic field should be represented by a superposition of modes that satisfy the boundary conditions on the metallic walls. In principle an infinite number of such modes is required. However, as long as the vacuum wavelength is about 5 times larger than the aperture width, the first mode [transverse electric and magnetic (TEM)] is sufficient for most practical purposes. This assumption is by no means critical for the present analysis and the calculation is similar when a larger number of modes is required; however, we use it since it makes the presentation simpler. In order to quantify this statement let us give a simple example of a periodic disk loaded structure: consider the case when $R_{\text{ext}} = 15.9$ mm, $R_{\text{int}} = 9.0$ mm, the period of the system is 10.0 mm, and the disk is 5 mm wide. For this geometry it is required that the phase advance per cell be 120° at 9 GHz. With 39 spatial (longitudinal) Floquet harmonics, the lower cutoff frequency ($kL = 0$), using three modes (TEM, TM_{01} and TM_{02}) in the grooves, was calculated to be 8.206 GHz, with two modes (TEM and TM_{01}) 8.192 and 8.192 GHz when only the TEM mode was used. For the higher cutoff ($kL = \pi$) the calculated frequencies were 9.270, 9.229, and 9.229 GHz correspondingly. Thus in the regime of interest the typical error associated with the neglect of the higher modes in the grooves is expected to be of the order of 1% or less. Within the framework of this approximation we can write, for the magnetic vector potential in the grooves,

$$A_z^n(r, z; \omega) = D_n T_{0,n} \left[\frac{\omega}{c} r \right]. \quad (14)$$

D_n is the amplitude of the magnetic vector potential and

$$\begin{aligned} T_{0,n} \left[\frac{\omega}{c} r \right] &= J_0 \left[\frac{\omega}{c} r \right] Y_0 \left[\frac{\omega}{c} R_{\text{ext}, n} \right] \\ &\quad - Y_0 \left[\frac{\omega}{c} r \right] J_0 \left[\frac{\omega}{c} R_{\text{ext}, n} \right]; \end{aligned} \quad (15)$$

this specific functional form is dictated by the condition that the longitudinal electric field should vanish on the external wall ($r = R_{\text{ext}, n}$). Later we shall also use the first derivative of this function

$$\begin{aligned} T_{1,n} \left[\frac{\omega}{c} r \right] &= J_1 \left[\frac{\omega}{c} r \right] Y_0 \left[\frac{\omega}{c} R_{\text{ext}, n} \right] \\ &\quad - Y_1 \left[\frac{\omega}{c} r \right] J_0 \left[\frac{\omega}{c} R_{\text{ext}, n} \right], \end{aligned} \quad (16)$$

where $J_0(x)$, $J_1(x)$, $Y_0(x)$, and $Y_1(x)$ are the zero and first order Bessel functions of the first and second kind. In the output arm, the magnetic vector potential reads

$$A_z(r, z; \omega) = D_N H_0^{(2)} \left[\frac{\omega}{c} r \right], \quad (17)$$

where $H_0^{(2)}(x)$ is the zero order Hankel function of the

second kind. Again, the functional form is dictated by the boundary conditions, which in this case assume no reflected wave along the output arm.

In order to determine the various amplitudes we next impose the boundary conditions following a method that resembles the one used in periodic structures. The main difference is that we no longer consider a single cell to characterize the entire system, but rather, examine each individual region. From the condition of continuity of the longitudinal electric field we can conclude that

$$A(k)I_0(\Delta) + B(k)K_0(\Delta) = -\frac{1}{2\pi} \frac{\alpha^2}{\Delta^2} \sum_{n=1}^N D_n \psi_{0,n} d_n L_n(k), \quad (18)$$

where $\alpha = (\omega/c)R_{\text{int}}$ is the normalized angular frequency, $\Delta = \Gamma R_{\text{int}}$ is the normalized wave number in the radial direction, and

$$L_n(k) = \frac{1}{d_n} \int_{z_n - d_n/2}^{z_n + d_n/2} dz 1 e^{jkz} \quad (19)$$

is the normalized spatial Fourier transform of the first mode amplitude (whose amplitude is constant) in the domain of the n th aperture. The function

$$\psi_{\nu,n} = \begin{cases} H_{\nu}^{(2)}(\alpha) & \text{for } n = N, \\ T_{\nu,n}(\alpha) & \text{for } n \neq N, \end{cases} \quad (20)$$

is the generalized (radial) modal function evaluated at the internal radius and n th aperture; $\nu (=0, 1)$ is the order of the function. In addition, z_n is the location of the center of the n th groove or arm and d_n is the corresponding width.

Imposing the continuity of the tangential magnetic field at each aperture (grooves and arm) we find

$$D_n \psi_{1,n} = -\frac{1}{\alpha} \int_{-\infty}^{\infty} dk [A(k)I_1(\Delta) - B(k)K_1(\Delta)] \Delta L_n^*(k). \quad (21)$$

$$\sigma_{s,n}(z) \equiv \frac{1}{d_n} \int_{z_n - d_n/2}^{z_n + d_n/2} d\xi e^{-\Gamma_s |\xi - z|}$$

$$= \begin{cases} e^{-\Gamma_s |z - z_n|} \text{sinhc}(\Gamma_s d_n / 2) & \text{for } |z - z_n| > d_n / 2 \\ 2\{1 - e^{-\Gamma_s d_n / 2} \cosh[\Gamma_s (z - z_n)]\} / \Gamma_s d_n & \text{for } |z - z_n| < d_n / 2, \end{cases} \quad (27)$$

is the projection of Green's function (s mode) on the n th aperture; $\text{sinhc}(x) = \sinh(x)/x$ and $\Delta_s^2 = p_s^2 - \alpha^2$. The other component is the discrete spectrum filling factor

$$F_s \equiv 2J_1(p_s R_b / R_{\text{int}}) / (p_s R_b / R_{\text{int}}). \quad (28)$$

To determine the amplitudes in Eq. (23) one has to multiply the source term by the inverse of the matrix τ defined by

$$\tau_{n,m} = \psi_{1,n} \delta_{n,m} - \psi_{0,m} \chi_{n,m}. \quad (29)$$

In these expressions

$$B(k) = \frac{\mu_0}{2\pi} \int_0^{R_b} dr' r' I_0(\Gamma r') \int_{-\infty}^{\infty} dz' e^{jkz'} J_2(r', z', \omega) \quad (22)$$

is the spatial Fourier transform of the current density averaged over the transverse direction with a weighting function that is proportional to the longitudinal electric field.

It is now convenient to substitute Eq. (18) in Eq. (21) in order to represent the entire electromagnetic problem in terms of the amplitudes of the mode in the grooves and output arm, i.e.,

$$\sum_{m=1}^N \tau_{n,m} D_m = S_n. \quad (23)$$

The source term

$$S_n = -\frac{\mu_0 I}{2\pi \alpha} a_n \quad (24)$$

is proportional to the average current and the Fourier transform of the normalized current density,

$$a_n = \frac{1}{R_{\text{int}}} \int_{-\infty}^{\infty} dz f_n(z) \langle e^{-j\omega\tau_i(z)} \rangle. \quad (25)$$

The Fourier transform is, with respect to a function,

$$f_n(z) = \sum_{s=1}^{\infty} \frac{p_s F_s}{\Delta_s J_1(p_s)} \sigma_{s,n}(z), \quad (26)$$

which is associated with the n th aperture. In particular if all the modes in the inner cylinder (index s) are below cutoff, this function peaks in the center of the aperture; p_s are the zeros of the zero order Bessel function of the first kind, i.e., $J_0(p_s) = 0$. The function $f_n(z)$ is the product of two components,

In this expression

$$\chi_{n,m} \equiv \frac{d_m \alpha}{2\pi} \int_{-\infty}^{\infty} dk \frac{I_1(\Delta)}{\Delta I_0(\Delta)} L_n^*(k) L_m(k), \quad (30)$$

the integral over k can be evaluated exactly by substituting the explicit expressions for $L_n(k)$ and using the Cauchy residue theorem [12,13]. This quantity represents the projection of Green's function (of a uniform waveguide) on two apertures:

$$\chi_{n,m} \propto \sum_{s=1}^{\infty} \cdots \frac{1}{d_n} \int_{z_n-d_n/2}^{z_n+d_n/2} dx_1 \frac{1}{d_m} \times \int_{z_m-d_m/2}^{z_m+d_m/2} dx_2 e^{-\Gamma_s |x_1-x_2|} . \quad (31)$$

Its exact evaluation reads

$$\chi_{n,m} = \frac{\alpha}{R_{\text{int}}^2} \sum_{s=1}^{\infty} \times \begin{cases} \frac{2}{\Gamma_s^2} [1 - e^{-\Gamma_s d_n/2} \text{sinhc}(\Gamma_s d_n/2)] & n=m, \\ \frac{d_m}{\Gamma_s} e^{-\Gamma_s |z_n-z_m|} \text{sinhc}(\Gamma_s d_n/2) & \\ \times \text{sinhc}(\Gamma_s d_m/2) & \text{otherwise,} \end{cases} \quad (32)$$

and $\Gamma_s^2 = (p_s/R_{\text{int}})^2 - (\omega/c)^2$. The electromagnetic problem has now been simplified to the inversion of a matrix whose components are analytic functions without *a priori* assumption on the form of the electromagnetic field.

EFFECTIVE ELECTRIC FIELD

The motion of the electrons is determined by the longitudinal electric field averaged over the beam cross section

$$E_{\text{SC}}(z) = -\frac{1}{j\omega\epsilon_0} \int_{-\infty}^{\infty} dz' J(z') \frac{1}{2\pi} \int_{-\infty}^{\infty} dk e^{-jk(z-z')} \left[1 - 2 \frac{I_1(\Delta_b)}{I_0(\Delta)} [I_0(\Delta)K_1(\Delta_b) + K_0(\Delta)I_1(\Delta_b)] \right] \quad (36)$$

and the "pure" electromagnetic term

$$E_{\text{EM}}(z) = \frac{-j\omega}{2\pi} \int_{-\infty}^{\infty} dk e^{-jkz} \frac{1}{I_0(\Delta)} F(k) \times \sum_{n=1}^N D_n d_n L_n(k) \psi_{0,n}, \quad (37)$$

where $F(k) \equiv 2I_1(\Delta_b)/\Delta_b$ is the (continuous spectrum) filling factor and $\Delta_b = \Gamma R_b$.

It can be seen that the grooves have no explicit effect on the space-charge term; in the Appendix we take advantage of this fact to show that

$$E_{\text{SC}}(z; \omega) \simeq -\frac{1}{j\omega\epsilon_0} \xi_{\text{SC}} J(z) = -j\eta_0 I \xi_{\text{SC}} \frac{c}{\omega} \frac{1}{\pi R_b^2} \langle e^{-j\omega\tau_i(z)} \rangle, \quad (38)$$

where

$$\xi_{\text{SC}} \equiv 1 - \sum_{s=1}^{\infty} \left[\frac{J_1(p_s R_b/R_{\text{int}})}{\Delta_s J_1(p_s)} \right]^2 \quad (39)$$

is the simplified plasma frequency reduction factor and $\eta_0 = \sqrt{\mu_0/\epsilon_0}$. The electromagnetic term can also be simplified [12,13] by substituting the explicit expression

$[E(z)]$ as defined in Eq. (7). In this section we shall use Eq. (23) to simplify the relation between the normalized current density and $E(z)$. The longitudinal component of the electric field is related to the magnetic vector potential by

$$E_z(r, z; \omega) = \frac{c^2}{j\omega} \left[\frac{\omega^2}{c^2} + \frac{\partial^2}{\partial z^2} \right] A_z(r, z; \omega), \quad (33)$$

which after substituting Eq. (9) reads

$$E_z(r, z; \omega) = \frac{c^2}{j\omega} \left[-\mu_0 J_z(r, z; \omega) - \frac{1}{r} \frac{\partial}{\partial r} r \frac{\partial}{\partial r} A_z(r, z; \omega) \right]. \quad (34)$$

Thus according to the definition of the effective electric field in Eq. (7), we have

$$E(z) = \frac{c^2}{j\omega} \left\{ -\mu_0 J(z) - \frac{2}{R_b} \left[\frac{\partial}{\partial r} A_z(r, z; \omega) \right]_{r=R_b} \right\}. \quad (35)$$

At this stage, we substitute the explicit expression for the magnetic vector potential in Eq. (11). The result has two contributions: the space-charge term

for $L_n(k)$ and using the Cauchy residue theorem; the result reads

$$E_{\text{EM}}(z) = \frac{\eta_0 I}{R_{\text{int}}} \sum_{n=1}^N f_n(z) \left[\sum_{m=1}^N T_{n,m} a_m \right], \quad (40)$$

where

$$T_{n,m} = \frac{j}{2\pi} \frac{d_n}{R_{\text{int}}} \psi_{0,n} [\tau^{-1}]_{n,m} \quad (41)$$

and it can be considered as a "discrete" Green function of the system since a_m is the Fourier transform of the normalized current density with respect to the function $f_m(\xi)$.

DYNAMICS

Now that the relation between the effective electric field acting on the particles and the current density has been established,

$$E(z) = E_{\text{SC}}(z) + E_{\text{EM}}(z), \quad (42)$$

we proceed to analyze of the beam-wave interaction. Substituting this effective field in the single particle energy conservation, defining $\xi_{\text{SC}} = \xi_{\text{SC}}(R_{\text{int}}/R_b)^2 \alpha \pi$ and $\bar{I} = \eta_0 I e/mc^2$, we obtain

$$\frac{d}{dz} \gamma_i = -\frac{1}{2R_{\text{int}}} \left[e^{j\omega\tau_i(z)} \left(-j\bar{I} \xi_{\text{SC}} \langle e^{-j\omega\tau_v(z)} \rangle_v + \bar{I} \sum_{n,m=1}^N T_{n,m} a_m f_n(z) \right) + \text{c.c.} \right]. \quad (43)$$

This is an integro-differential equation that describes the dynamics of the electrons, and in order to determine γ_i at any given location it is necessary to know the Fourier transform of the normalized current density a_n , which in turn requires knowledge of the trajectories of all particles over the entire interaction region; see Eq. (25).

Before we proceed to actually present a solution of this set of equations it is important to make two comments that are evident from Eq. (43) and our prior definitions:

(i) Global energy conservation implies

$$\langle \gamma_i(\infty) \rangle - \langle \gamma_i(-\infty) \rangle = -\frac{1}{2} \bar{I} \sum_{n,m=1}^N a_n^* Z_{n,m} a_m, \quad (44)$$

where

$$Z_{n,m} = \frac{1}{2} [T_{n,m} + T_{m,n}^*] \quad (45)$$

is the *interaction impedance matrix*. This expression infers that in the case of nonadiabatic changes from periodicity, namely, in quasiperiodic structures, we can no longer refer to the interaction impedance as a scalar (and local) quantity but rather as a matrix, and the interaction at a given location is affected by the geometry elsewhere. Furthermore, since the left-hand side of the global energy conservation [Eq. (44)] is proportional to the overall efficiency, it is evident that the latter is controlled by the interaction impedance matrix. In the example presented next, it will be shown that it is the largest eigenvalue of this matrix that determines the efficiency of the interaction.

(ii) the space-charge term has no explicit effect on the global energy conservation. Furthermore, in the case of a very peaked distribution (e.g., a single macroparticle) it has no effect on the equations of motion.

In order to solve the integro-differential equation in Eq. (43) for a large number of macroparticles (more than 30 000 were used), an iterative way was chosen. Typically a simple distribution is assumed, enabling the calculation of the zero interaction $a_n^{(0)}$. With this quantity, the trajectories of all particles are calculated, and in parallel, the “new” $a_n^{(1)}$ is evaluated; at the end of the iteration the two a_n 's are compared. If the relative error is less than 1% the simulation is terminated. Otherwise we calculate the equations of motion again but this time using $a_n^{(1)}$ to determine the dynamics of the particles and calculate $a_n^{(2)}$ in parallel. Typically if the energy spread of the electrons at the input is not too large, then 3–4 iterations are sufficient for convergence.

Consider now a modulated beam that drives an output structure. The initial energy of the electrons is 850 keV and the structure should extract 70% of their kinetic energy; for the zero order design let us assume that in the interaction region there is only a single macroparticle at a time. Furthermore, the disk thickness is taken to be 1 mm in order to ensure maximum group velocity. For the same reason the phase advance per cell is taken to be 90° . In the design process, the total interaction length and each aperture is determined assuming that the velocity of a single macroparticle varies in space according to

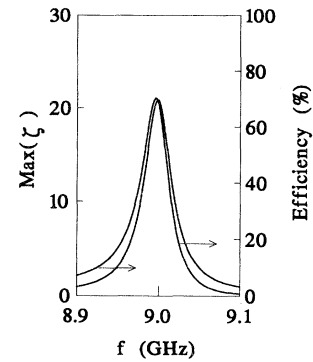


FIG. 2. Largest eigenvalue of the interaction impedance matrix as a function of the frequency. Overlaid is also the efficiency calculated assuming all the electrons form a single macroparticle.

$$V(z) = V(0)/(1 + qz); \quad (46)$$

q and the total interaction length d_{tot} are determined from the required efficiency and the condition of a single macrobunch in the interaction region. For simplicity, we assume that the internal and external radius are the same in all cells. Their value is determined by *maximizing the largest eigenvalue of the interaction impedance matrix* at 9 GHz, as illustrated in Fig. 2 where $R_{\text{int}} = 9$ mm and $R_{\text{ext}} = 16.47$ mm; the other geometrical parameters are $d_1 = 6.5$ mm, $d_2 = 6.0$ mm, $d_3 = 5.7$ mm, and $d_4 = 5.4$ mm. Overlaid is also the efficiency assuming a single macroparticle injected into the system in one period of the wave. The dynamics of the particle is calculated numerically [Eq. (43)].

The efficiency of the electromagnetic energy conversion is strongly dependent on the phase-space distribution at the input, as indicated in Fig. 3; the phase here is defined as $\chi_i(z) \equiv \omega\tau_i(z)$. For a perfectly bunched beam the efficiency is as designed (for $I = 300$ A). However, as the initial phase distribution increases to $-45^\circ < \chi(0) < 45^\circ$ the efficiency drops to 45% and to 25% for $-90^\circ < \chi(0) < 90^\circ$; it drops to virtually zero for a uniform distribution.

An interesting feature is revealed in Fig. 4 where we

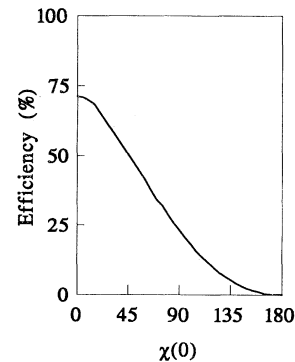


FIG. 3. Efficiency as a function of the initial phase distribution at the input.

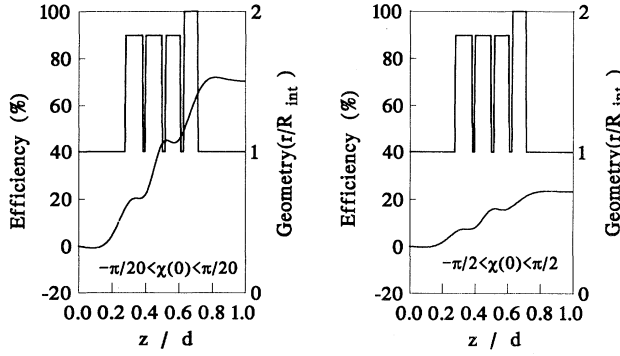


FIG. 4. Variation of the efficiency in space for a narrow $[-9^\circ < \chi(0) < 9^\circ]$ initial phase distribution and a broad one $[-90^\circ < \chi(0) < 90^\circ]$. The slope is different, but the other general characteristics are preserved.

present the variation in space of the efficiency for two initial distributions: $-9^\circ < \chi(0) < 9^\circ$ and $-90^\circ < \chi(0) < 90^\circ$. We observe that the general pattern is virtually identical in both cases and only the spatial growth rate is smaller. The reduced efficiency is a result of energy transferred back to electrons that are actually accelerated, as illustrated in Fig. 5; clearly in the narrower initial phase-space distribution all the electrons are decelerated at the output, whereas in the case of broader distribution a substantial fraction of electrons is accelerated.

Finally, the efficiency is illustrated in Fig. 6 as a function of the frequency for $-15^\circ < \chi(0) < 15^\circ$; the curve is virtually identical to that of the single macroparticle case (Fig. 3). Overlaid, we present the energy spread ($\Delta\gamma \equiv \sqrt{\langle \gamma^2 \rangle - \langle \gamma \rangle^2}$) at the output; up to a constant value, this quantity varies as the derivative of the efficiency with respect to the frequency.

SUMMARY

We have presented a semianalytical approach that enables the design and analysis of quasiperiodic structures.

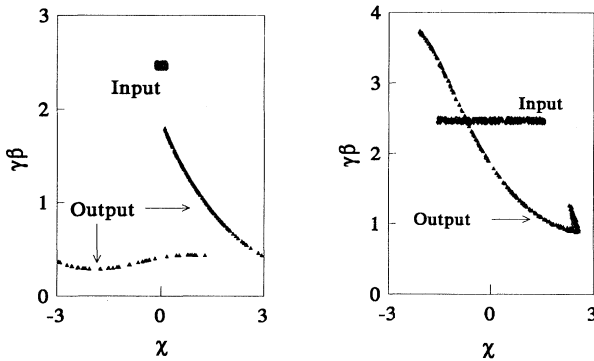


FIG. 5. Phase space for a narrow, $-9^\circ < \chi(0) < 9^\circ$, distribution in the left frame and broad one in the right $[-90^\circ < \chi(0) < 90^\circ]$. In the narrow case all electrons are decelerated, whereas in the broader case a fraction of the electrons are accelerated and consequently, the efficiency is lower, as also indicated in Fig. 4.

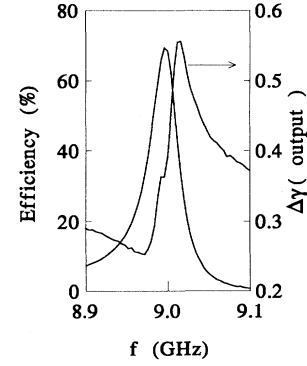


FIG. 6. Efficiency as a function of the frequency for a phase distribution of $-15^\circ < \chi(0) < 15^\circ$; the resemblance to the single macroparticle case in Fig. 2 is evident. Overlaid is the energy spread at the output; up to a constant value it behaves like the derivative of the efficiency.

The model consists of a set of pill-box cavities and one or more output arms attached to a cylindrical waveguide. The electromagnetic problem is formulated in terms of Green's function, which can be calculated analytically. With this function, the longitudinal field that acts on the particles is evaluated, and therefore the beam-wave interaction is formulated in a self-consistent way [Eq. (43)], without a *a priori* assumption regarding the form of the electromagnetic wave.

In the framework of this formulation the interaction impedance, which in a uniform structure is a scalar function, becomes a matrix. It was shown that the design of geometric parameters for a high-efficiency traveling wave output section relies on the optimization of the largest eigenvalue of this matrix at the required frequency.

The beam-wave interaction is a solution of Eq. (43) for a given initial particle distribution (χ). The performance of a 70% efficiency system was presented and a similar design is possible for 80%. Above 90% efficiency, simulations indicate that there are always reflected electrons for any practical phase-space distribution and this violates our assumption associated with Eq. (3).

ACKNOWLEDGMENTS

The author has benefited from fruitful discussions with Professor John A. Nation. This work was supported by the U.S. Department of Energy and the U.S.-Israel Binational Science Foundation.

APPENDIX

To evaluate the space-charge term in a uniform waveguide we start with Green's function associated with TM_{0s} modes in a cylindrical waveguide,

$$G_{\omega}(r, z | r', z') = \sum_{s=1}^{\infty} \frac{J_0(p_s r / R_{\text{int}}) J_0(p_s r' / R_{\text{int}})}{\frac{1}{2} R_{\text{int}}^2 J_1^2(p_s)} \frac{1}{4\pi\Gamma_s} e^{-\Gamma_s |z-z'|}. \quad (\text{A1})$$

Using the same method as in Eqs. (31)–(33) we obtain

$$E(z) = \frac{-1}{j\omega\epsilon_0} \left[J(z) - \frac{1}{R_{\text{int}}} \int_{-\infty}^{\infty} dz' J(z') \sum_{s=1}^{\infty} e^{-\Gamma_s |z-z'|} \frac{1}{2\Delta_s} \left[\frac{2J_1(p_s R_b / R_{\text{int}})}{J_1(p_s)} \right]^2 \right], \quad (\text{A2})$$

which can be simplified if all electromagnetic modes are below the cutoff and in particular, for the case when the current density $|J(z)|$ varies much slower than $e^{-\Gamma_s |z-z'|}$. Subject to these assumptions, we can assume that the main contribution to the integral is from the region $z = z'$ and therefore $J(z)$ can be extracted from the integral. The result in this case reads

$$E(z) = \frac{-1}{j\omega\epsilon_0} J(z) \left[1 - \sum_{s=1}^{\infty} \left[\frac{J_1(p_s R_b / R_{\text{int}})}{\Delta_s J_1(p_s)} \right]^2 \right] \quad (\text{A3})$$

or

$$E_{\text{SC}}(z; \omega) = -\frac{1}{j\omega\epsilon_0} \xi_{\text{SC}} J(z), \quad (\text{A4})$$

where the space-charge coefficient ξ_{SC} is given by

$$\xi_{\text{SC}} = 1 - \sum_{s=1}^{\infty} \left[\frac{J_1(p_s R_b / R_{\text{int}})}{\Delta_s J_1(p_s)} \right]^2, \quad (\text{A5})$$

as indicated in Eq. (39).

-
- [1] M. A. Allen, J. K. Boyd, R. S. Callin, H. Deruyter, K. R. Epply, K. S. Faust, W. R. Fowkes, J. Haimson, H. A. Hoag, D. B. Hopkins, T. Houck, R. F. Koontz, T. L. Lavine, G. A. Loew, B. Mecklenburg, R. H. Miller, R. D. Ruth, R. D. Ryne, A. M. Sessler, A. E. Vleiks, J. W. Wang, G. A. Gestenskow, and S. S. Yu, *Phys. Rev. Lett.* **63**, 2472 (1989).
- [2] E. Kuang, T. J. Davis, G. S. Kerslick, J. A. Nation, and L. Schächter, *Phys. Rev. Lett.* **71**, 2666 (1993).
- [3] J. Haimson and B. Mecklenburg, in *Intense Microwave and Particle Beams III*, edited by H. E. Brandt, SPIE Proceedings Vol. 1629 (SPIE, Bellingham, WA, 1992), p. 209.
- [4] V. E. Balakin, in *XVth International Conference on High Energy Accelerators (HEACC'92) Hamburg, Germany*, [Int. J. Mod. Phys. A **2**, 784 (1993)].
- [5] D. A. Shiffler, J. A. Nation, and C. B. Wharton, *Appl. Phys. Lett.* **54**, 674 (1989).
- [6] D. A. Shiffler, J. A. Nation, J. D. Ivers, G. S. Kerslick, and L. Schächter, *Appl. Phys. Lett.* **58**, 899 (1991).
- [7] D. A. Shiffler, J. A. Nation, J. D. Ivers, G. S. Kerslick, and L. Schächter, *J. Appl. Phys.* **70**, 106 (1991).
- [8] L. Schächter, J. A. Nation, and D. A. Shiffler, *J. Appl. Phys.* **70**, 114 (1991).
- [9] L. Schächter and J. A. Nation, *Phys. Rev. A* **45**, 8820 (1992).
- [10] L. Schächter, *Phys. Rev. A* **43**, 3785 (1991).
- [11] N. M. Kroll, P. L. Morton, and M. N. Rosenbluth, *IEEE Quantum Electronics QE-17*, 1436 (1981).
- [12] L. Schächter and J. A. Nation, *Appl. Phys. Lett.* **63**, 2441 (1993).
- [13] L. Schächter and J. A. Nation, *Phys. Plasmas* (to be published).